

A Histone Methylation Network Regulates Transgenerational Epigenetic Memory in *C. elegans*

Eric L. Greer,^{1,2} Sara E. Beese-Sims,^{3,6} Emily Brookes,^{1,2,6} Ruggero Spadafora,² Yun Zhu,⁴ Scott B. Rothbart,⁵ David Aristizábal-Corrales,^{1,2} Shuzhen Chen,^{1,2} Aimee I. Badeaux,^{1,2} Qiuye Jin,^{1,2} Wei Wang,⁴ Brian D. Strahl,⁵ Monica P. Colaiácovo,³ and Yang Shi^{1,2,*}

¹Department of Cell Biology, Harvard Medical School, Boston, MA 02115, USA

²Division of Newborn Medicine, Children's Hospital Boston, 300 Longwood Avenue, Boston, MA 02115, USA

³Department of Genetics, Harvard Medical School, Boston, MA 02115, USA

⁴Department of Chemistry and Biochemistry, University of California, San Diego, La Jolla, CA 92093, USA

⁵Department of Biochemistry and Biophysics, Lineberger Comprehensive Cancer Center, The University of North Carolina at Chapel Hill School of Medicine, Chapel Hill, NC 27599, USA

⁶These authors contributed equally to this work

*Correspondence: yshi@hms.harvard.edu

<http://dx.doi.org/10.1016/j.celrep.2014.02.044>

This is an open access article under the CC BY license (<http://creativecommons.org/licenses/by/3.0/>).

SUMMARY

How epigenetic information is transmitted from generation to generation remains largely unknown. Deletion of the *C. elegans* histone H3 lysine 4 dimethyl (H3K4me₂) demethylase *spr-5* leads to inherited accumulation of the euchromatic H3K4me₂ mark and progressive decline in fertility. Here, we identified multiple chromatin-modifying factors, including H3K4me₁/me₂ and H3K9me₃ methyltransferases, an H3K9me₃ demethylase, and an H3K9me reader, which either suppress or accelerate the progressive transgenerational phenotypes of *spr-5* mutant worms. Our findings uncover a network of chromatin regulators that control the transgenerational flow of epigenetic information and suggest that the balance between euchromatic H3K4 and heterochromatic H3K9 methylation regulates transgenerational effects on fertility.

INTRODUCTION

Most heritable information is transmitted by DNA, following Mendelian inheritance (Avery et al., 1944), but some traits, such as longevity, fertility, disease susceptibility, and obesity, can be inherited nongenetically in several model organisms (Daxinger and Whitelaw, 2012; Greer and Shi, 2012; Youngson and Whitelaw, 2008). The underlying molecular mechanisms of transgenerational epigenetic transmission remain unclear, but chromatin changes may play a role.

Chromatin is composed of 146 base pairs of DNA wrapped around a histone octamer (two copies each of histone H2A, H2B, H3, and H4). Both DNA and histones are modified, which impacts chromatin-templated processes. Among many histone modifications, lysine (K) methylation is of particular interest in the context of epigenetic inheritance as this modification is

more stable but can also be dynamically regulated. Histone methylation can be associated with either transcriptional activation or repression. For instance, histone H3K4 di- and trimethylation (H3K4me₂/me₃) are associated with active or poised gene transcription (Bernstein et al., 2002; Pokholok et al., 2005; Santos-Rosa et al., 2002), whereas H3K9 di- and trimethylation (H3K9me₂/me₃) are associated with transcriptional repression, gene silencing, and heterochromatin (Bannister et al., 2001; Ebert et al., 2006; Li et al., 2007). Both H3K4 and H3K9 methylation events are regulated by multiple, site-specific methyltransferases and demethylases (Mosammamaparast and Shi, 2010; Ruthenburg et al., 2007). When H3K4 is methylated, H3K9 is often demethylated and sometimes acetylated; likewise, when H3K9 is methylated, H3K4 is often unmethylated (Barski et al., 2007; Guenther et al., 2007; Heintzman et al., 2007; Mikkelsen et al., 2007; Wang et al., 2008). Antagonism between H3K4 and H3K9 methylation plays a critical role in dictating the boundaries between euchromatin and heterochromatin (Lan et al., 2007; Rudolph et al., 2007). However, the functional consequences of the crosstalk between methylation at H3K4 and H3K9 remain incompletely understood.

SPR-5, the *C. elegans* ortholog of the human H3K4me₁/me₂-specific demethylase LSD1, regulates transgenerational inheritance. *C. elegans* without *spr-5* do not exhibit sterility initially, but successive generations lacking *spr-5* display increasing infertility concomitant with global accumulation of H3K4me₂ (Katz et al., 2009; Nottke et al., 2011). This progressive phenotype can be reversed by the addition of a single copy of *spr-5*. However, how this epigenetic memory is transmitted across generations is still unknown. To investigate the underlying molecular mechanism of these inherited epigenetic changes, we carried out targeted RNAi screens to identify suppressors and enhancers of the progressive fertility phenotypes associated with loss of *spr-5*. Our findings not only uncovered a network of enzymes and reader proteins involved in regulating H3K4 and H3K9 methylation but also demonstrated that a functional interplay between H3K4 and H3K9 methylation plays a key role in regulating epigenetic inheritance in *C. elegans*.

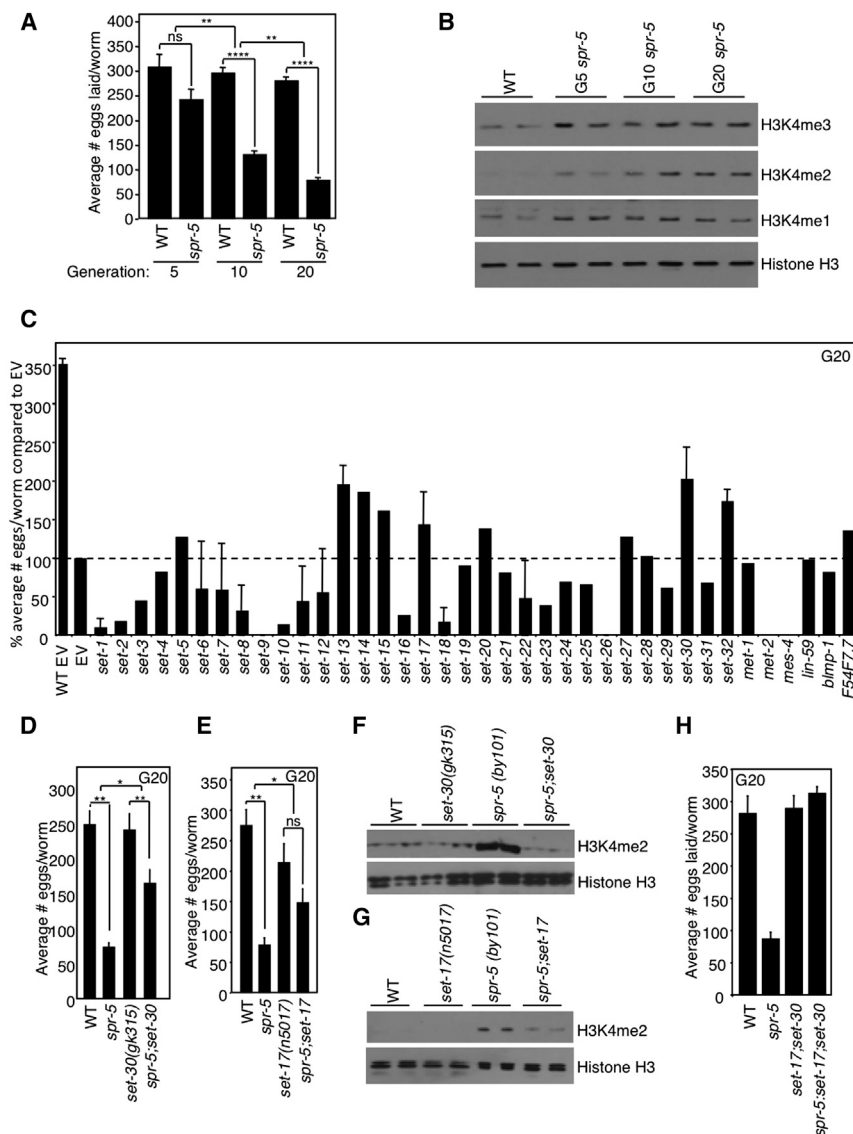


Figure 1. *set-17* and *set-30* Deletions Suppress the Progressive Sterility of *spr-5* Mutant Worms

(A) *spr-5(by101)* mutant worms display progressive fertility defects (bars represent mean \pm SEM for four experiments for generation 5, 15 experiments for generation 10, and 34 experiments for generation 20: each experiment consists of average eggs laid for ten worms of each genotype performed in triplicate).

(B) H3K4me2 increases across generations of *spr-5(by101)* mutant worms as assessed by whole-worm western blots of L4-stage worms. H3K4me1 and H3K4me3 are higher in *spr-5(by101)* mutant worms but do not change across generations. Blots are representative of four independent experiments performed in duplicate.

(C) Number of eggs laid by *spr-5(by101)* mutant worms fed dsRNA of *C. elegans* potential methyltransferases or empty vector (EV) for 20 generations.

(D) *spr-5;set-30* double mutants for 20 generations causes a partial suppression of decreased fertility capacity of *spr-5(by101)* mutant worms. This graph displays the mean \pm SEM of four independent experiments: each experiment consists of average eggs laid for ten worms of each genotype performed in triplicate.

(E) *spr-5;set-17* double mutant worms have a partial suppression of the fertility defect of *spr-5(by101)* mutant worms at generation 20. This graph displays the mean \pm SEM of four independent experiments.

(F) *spr-5(by101)* mutant worms have increased H3K4me2 at generation 20, but *spr-5;set-30* double mutants have normal H3K4me2 levels as assessed by whole-worm western blots of L3 worms.

(G) *spr-5;set-17* double mutants have lower H3K4me2 at generation 20 than *spr-5(by101)* mutants as assessed by whole-worm western blots of L4 worms.

(H) *spr-5;set-17;set-30* triple-mutant worms have a complete suppression of the fertility defect of *spr-5(by101)* mutant worms at generation 20. This graph displays the mean \pm SEM of three independent experiments: each experiment consists of average eggs laid for ten worms of each genotype performed in triplicate. * $p < 0.05$, ** $p < 0.01$, **** $p < 0.0001$.

RESULTS

The Main RNAi Pathways Mediated by *rde-1* and *ergo-1* Are Not Involved in the Progressive Sterility of *spr-5(by101)* Mutant Worms

Genetic ablation of the H3K4me2 demethylase *spr-5* in *C. elegans* leads to a progressive decrease in fertility and increase in H3K4me2 over generations (Katz et al., 2009; Nottke et al., 2011). We confirmed the progressive loss of fertility, assessed by counting laid eggs, in successive generations of worms using two genetically null deletion strains of *spr-5* (*spr-5(by101)* and *spr-5(by134)*) (Figures 1A and S1A), but for the remainder of the studies, we focused on the *spr-5(by101)* allele. We observed a generational accumulation of H3K4me2 in *spr-5(by101)* mutant worms (Figure 1B). In contrast, H3K4me1 and H3K4me3 levels,

though elevated in *spr-5(by101)* mutant worms, did not change across generations.

As RNAi inheritance has been implicated in transgenerational epigenetic inheritance in several species (Moazed, 2011), we first investigated whether RNAi pathways played a role in *spr-5*-induced epigenetic inheritance. The argonaute genes *rde-1* and *ergo-1* are largely required for exogenous and endogenous RNAi in *C. elegans*, respectively (Grishok et al., 2000; Yigit et al., 2006), although other argonautes in *C. elegans* could be required for specific RNA inheritance events (Conine et al., 2013). Worms carrying double mutations of *spr-5(by101)* with either *rde-1* or *ergo-1* laid the same number of eggs as *spr-5(by101)* at generation 10 (Figures S1B and S1C), suggesting that RNAi inheritance mediated by these argonautes does not play a role in the generational sterility inheritance of *spr-5* mutants.

SET-17 and SET-30 Suppress Transgenerational Phenotypes of the *spr-5(by101)* Mutant Worms

Because SPR-5 is an H3K4me1/me2 demethylase, we hypothesized that H3K4me2-specific methylases would act as suppressors. These enzymes are unknown in *C. elegans*, so we knocked down all genes containing predicted methyltransferase domains (Andersen and Horvitz, 2007; Herz et al., 2013) (Figure 1C). *spr-5(by101)* mutant worms' fertility was assessed after being fed bacteria expressing double-stranded RNA (dsRNA) against 39 methyltransferase-domain-containing genes for 20 generations. Knockdown of *set-13*, *set-14*, *set-15*, *set-17*, *set-20*, *set-30*, and *set-32* all partially suppressed the progressive sterility of *spr-5(by101)* mutant worms. To rule out off-target effects, we crossed predicted null mutants of each of these genes with *spr-5* mutants and examined the effects. We found that mutations of *set-20* and *set-32* had no effect on the fertility of *spr-5(by101)* mutant worms (Figures S2A and S2B), suggesting the RNAi suppression was due to off-target effects. A predicted genetic-null mutation of *set-25*, which did not suppress the phenotype in our RNAi screen but is required for the maintenance of silencing triggered by Piwi-interacting RNA in some instances (Ashe et al., 2012), also had no effect on *spr-5(by101)* fertility (Figure S2C). We failed to obtain progeny from *spr-5;set-13* double mutants for reasons that are unclear (Figure S2D).

Importantly, maintaining either *set-17* or *set-30* as homozygous mutants for 20 generations significantly, albeit partially, suppressed *spr-5(by101)* transgenerational sterility (Figures 1D and 1E), confirming the initial RNAi screen results. Genetic ablation of either *set-17* or *set-30* also suppressed *spr-5(by101)*-elevated H3K4me2 levels (Figures 1F and 1G). Furthermore, deletion of both *set-17* and *set-30* in *spr-5(by101)* mutants completely suppressed the transgenerational sterility (Figure 1H). The closest mammalian homolog of SET-17 is PRDM9, which has been suggested to mediate H3K4me2/H3K4me3 (Hayashi et al., 2005) (full protein: 33.2% identity; SET domain: 46.67% identity). Collectively, these findings suggest that SET-17 and SET-30 are potential H3K4 methyltransferases.

SET-17 and SET-30 Are H3K4me1/me2 Methyltransferases

To determine whether SET-17 and SET-30 mediate H3K4 methylation, we performed in vitro radioactive methyltransferase assays using glutathione S-transferase (GST)-tagged SET-17 and SET-30, expressed and purified from bacteria. SET-17 specifically methylated histone H3 of calf thymus histones as well as unmodified recombinant histone H3 and an H3 peptide containing the first 21 amino acids (Figure 2A). Using histone-methyl-specific antibodies, we found SET-17 mediated mono- and dimethylation of H3K4 in calf thymus histone or recombinant H3 (Figures 2B and S3A) while displaying no activities toward other lysine residues (Figures 2B and S3A; data not shown). Furthermore, we found that SET-17 methylated unmodified H3 peptide and to a lesser extent the H3K4me1 premethylated peptide but did not methylate the H3K4me2 or H3K4me3 pre-methylated peptides (Figure 2C). In vivo, *set-17* mutant worms displayed lower global levels of H3K4me but wild-type levels of H3K27me2 (Figure 2D). Together, these results suggest that SET-17 is an H3K4me1/me2 methyltransferase.

Similar to SET-17, SET-30 preferentially mediates H3K4me1/me2 on calf thymus histones and 293T cell nucleosomes (Figures 2E and S3B). Unlike SET-17, SET-30 was unable to methylate recombinant histone substrates (data not shown). In vivo, early larval stage L1 and L2 (but not L3 and L4) *set-30* mutant worms displayed lower H3K4me levels (Figures 1F and 2F; data not shown), consistent with SET-30 being an H3K4 methyltransferase. Taken together, our results demonstrate that SET-17 and SET-30 mediate H3K4me1/me2 in vitro and in vivo and suggest that they may oppose the activity of the demethylase SPR-5. Combined deletion of *set-17* and *set-30* did not completely eliminate global H3K4 mono- and dimethylation (data not shown), suggesting the existence of additional H3K4 mono and dimethyltransferases.

Loss of SET-30, but Not SET-17, Reverts the Progressive Sterility of *spr-5* Mutant Worms

The above genetic suppression experiment involved simultaneous and persistent inhibition of SET-17 or SET-30 in *spr-5* worms from generation one. We wished to determine whether removal of *set-17* or *set-30* in later-generation *spr-5* mutants, which are already less fertile, is sufficient to revert the reproductive capacity. We therefore assessed *spr-5(by101)* mutants' fertility after being maintained for 20 generations on empty vector control RNAi (EV) bacteria and then switched to *set-17* or *set-30* RNAi for an additional five generations. *set-30*, but not *set-17*, RNAi partially reverted the *spr-5(by101)* progressive sterility and increased H3K4me2 levels (Figures 3A and 3B). The reversion became evident after two to three generations on *set-30* RNAi as *spr-5(by101)* mutant worms began to lay as many eggs as *spr-5(by101)* mutant worms fed *set-30* RNAi for all generations (Figure 3C). These results suggest that, whereas SET-17 may be required for initiating the transgenerational phenotypes, SET-30 might be important in both initiating and maintaining progressive sterility associated with the loss of SPR-5.

Loss of the Predicted H3K9 Mono/Dimethyltransferase MET-2 and the H3K9 Trimethyltransferase SET-26 Accelerate the Progressive Sterility and Accumulation of H3K4me2 in *spr-5* Mutant Worms

Our RNAi screen also identified genes whose knockdown accelerated the progressive sterility of *spr-5* mutants (Figure 1C). Knockdown of *set-9*, *set-26*, *met-2*, and *mes-4* had the strongest effect, rendering *spr-5* mutants completely sterile by generations 2–13. *mes-4* was previously identified as a sterility inducer after one generation in wild-type worms (Capowski et al., 1991). *met-2* mutants were previously reported to display a mortal germline phenotype after 18–28 generations (Andersen and Horvitz, 2007), whereas *set-9* and *set-26* have no reported fertility effects.

To confirm the RNAi result, we crossed the predicted null mutants, *met-2(ok2307)*, *met-2(n4256)*, *set-9(n4949)*, and *set-26(tm3526)*, with *spr-5(by101)* mutants. Crossing either *met-2* mutant with *spr-5* accelerated the progressive sterility such that *spr-5;met-2* double mutants were completely sterile by generation 2 (Figure 4A; data not shown). Interestingly, mutation of *set-26*, but not *set-9*, accelerated the progressive sterility

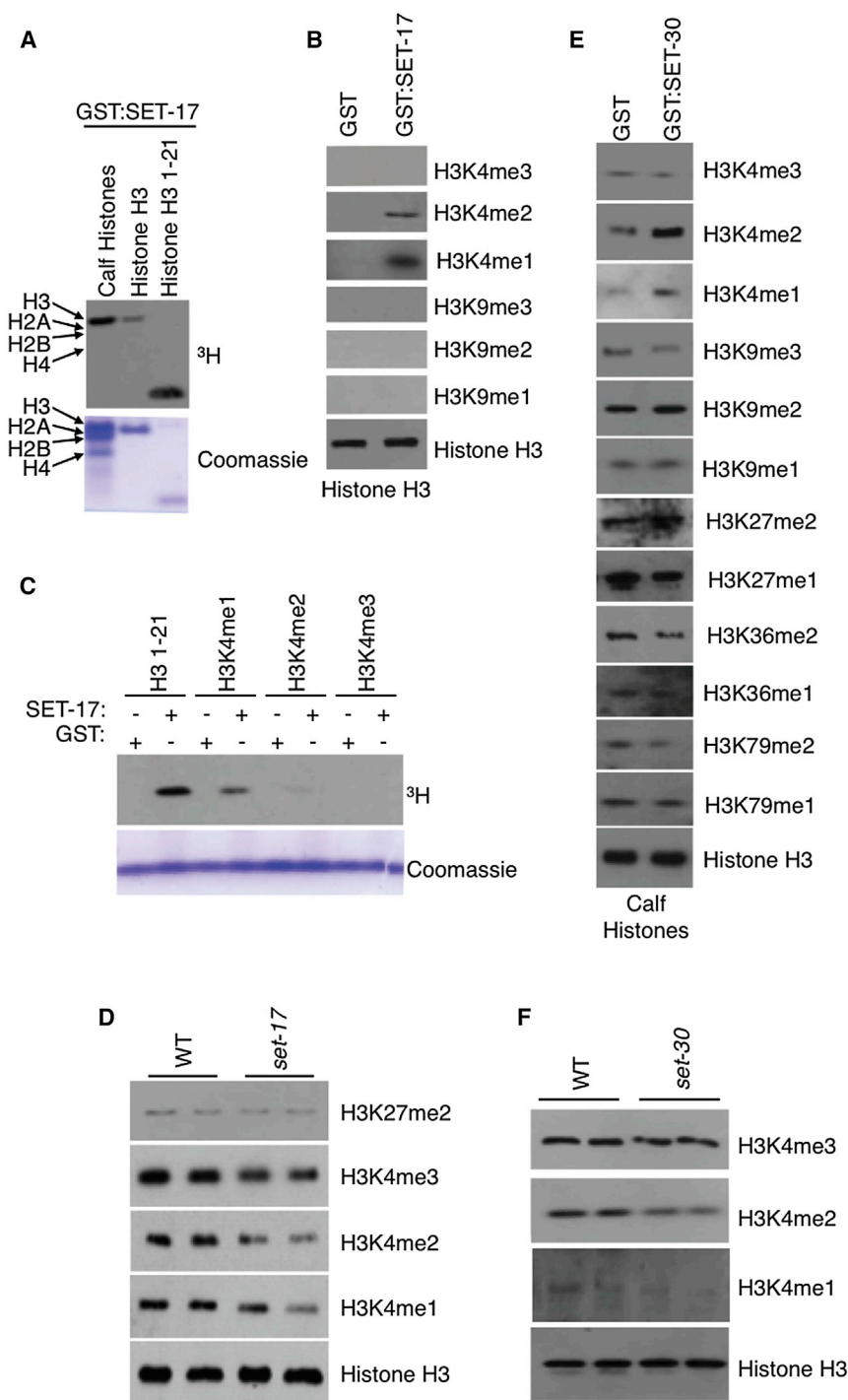


Figure 2. SET-17 and SET-30 Are H3K4me1/me2 Methyltransferases

(A) GST:SET-17 full-length protein methylates histone H3 amino acids 1–21, histone H3, and only histone H3 of calf histones *in vitro*. (B) GST:SET-17 full-length protein methylates H3K4me1/me2 of histone H3 as assessed by western blots of *in vitro* methylation assays performed on recombinant histone H3. (C) GST:SET-17 methylates H3K4me1 and H3K4me2 as assessed by radioactive methyltransferase assays of histone H3 amino acids 1–21, which are unmodified or premethylated on H3K4. (D) *set-17(n5017)* mutant worms have lower H3K4 methylation as assessed by whole-worm western blots of L4 worms. (E) GST:SET-30 full-length protein methylates H3K4me1/me2 as assessed by western blots of *in vitro* methylation assay performed on histones. (F) *set-30(gk315)* mutant worms have lower H3K4 methylation as assessed by whole-worm western blots of L1 worms.

progressive decline in fertility (Figure 4B), suggesting that *set-26* participates in fertility regulation specifically through genetic interactions with *spr-5*. Although *set-26* worms did not show elevated levels of H3K4me2, *spr-5;set-26* double mutants displayed significantly higher levels of H3K4me2 at generation 4 than *spr-5* mutants (Figure 4C).

Interestingly, *met-2*, *set-9*, and *set-26* are all predicted H3K9 methylases (Andersen and Horvitz, 2007; Bessler et al., 2010; Ni et al., 2012; Towbin et al., 2012). We performed *in vitro* radioactive methyltransferase assays using the catalytic SET domain of SET-26 (SET-26_{SET}) to identify its histone substrates. SET-26_{SET} selectively methylated H3, but not H2A, H2B, or H4 of 293T cell nucleosomes, but failed to methylate recombinant substrates (Figure S3C; data not shown). SET-26_{SET} mediated H3K9me3, but not methylation of other H3 lysine residues, suggesting that SET-26 is an H3K9 trimethyltransferase (Figures 4D and S3C). *met-2* mutants have lower H3K9me in embryos when assessed by mass spectrometry (Towbin et al., 2012) but have undetectable

of *spr-5* such that the *spr-5;set-26* double mutants were completely sterile by generations 5–8 (Figure 4B). The reason that we identified *set-9* as an enhancer in the RNAi screen was likely due to *set-9* small interfering RNA cross-inhibiting SET-26 expression, due to the high degree of sequence similarity between these two genes (97% sequence identity). Importantly, *set-26(tm3526)* mutation on its own did not cause a

H3K9me2 and high levels of H3K9me3 in the adult germline as assessed by immunofluorescence (Bessler et al., 2010). Therefore MET-2 has been proposed to be an H3K9 mono- and dimethyltransferase (Andersen and Horvitz, 2007; Bessler et al., 2010; Towbin et al., 2012), although its direct methyltransferase activity has not been biochemically demonstrated.

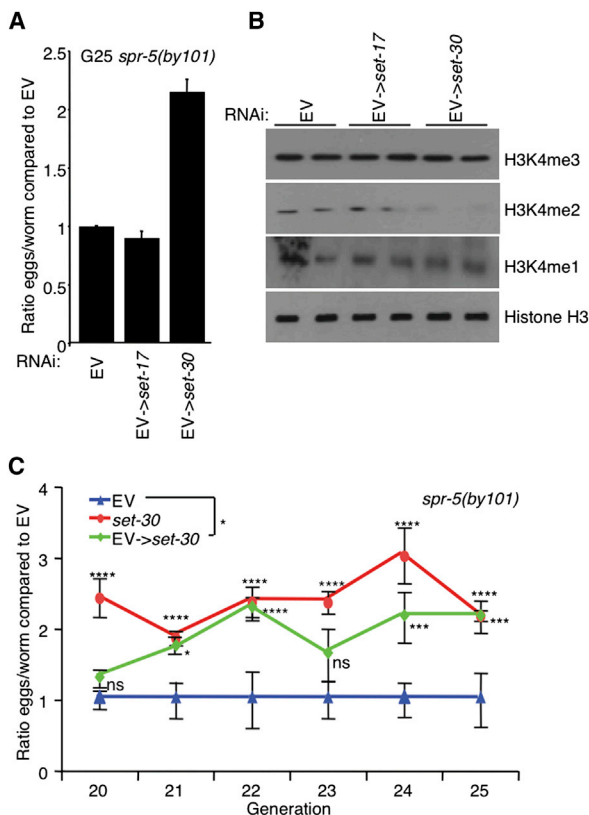


Figure 3. *set-30* Knockdown Reverts the Progressive Phenotypes of *spr-5* Mutant Worms

(A) RNAi against *set-30*, but not *set-17*, for five generations partially reverted the fertility defect of *spr-5(by101)* mutant worms fed EV for 20 generations prior. This graph represents the mean \pm SEM of three independent experiments: each experiment consists of average eggs laid for ten worms of each genotype performed in triplicate.

(B) *spr-5(by101)* mutant worms increased H3K4me2 at generation 25 are reverted by five generations of treatment with *set-30* RNAi as assessed by whole-worm western blots of L3 worms.

(C) The fertility defect of *spr-5(by101)* mutant worms fed EV for 20 generations and switched to *set-30* RNAi suggests that *set-30* knockdown for two to three generations causes the same degree of partial reversion of the fertility defect as *spr-5(by101)* mutant worms that had been fed dsRNA against *set-30* for 22 to 23 generations. * $p < 0.05$, *** $p < 0.001$, **** $p < 0.0001$.

Loss of the H3K9me3 Demethylase JMJD-2 Suppresses the Transgenerational Fertility Defects of *spr-5(by101)* Mutant Worms

If acceleration of the infertility of *spr-5* mutants upon loss of MET-2 and SET-26 depends on their function as H3K9 methylases, the absence of an H3K9 demethylase should suppress this defect. Among the 11 demethylase candidates (Klose et al., 2006), we found that only mutation of *jmjd-2(tm2966)*, which deletes the catalytic Jumonji C domain and should produce an enzymatically null protein, suppressed the *spr-5(by101)* progressive fertility defect (Figures 4E and S2E–S2I). JMJD-2 is a putative H3K9me3/H3K36me3 demethylase based on its sequence homology with the mammalian JMJD2 family of demethylases (Black et al., 2010; Whetstone et al., 2006). Consistently, we found that JMJD-2 demethylated

H3K9me3 and H3K36 methylation on calf histones, but not other H3 lysine residues (Figure 4F). Together, these results suggest that H3K9me3 regulates the transgenerational progressive sterility of *spr-5(by101)* mutant worms.

Indeed, we found that H3K9me3 levels in L4 *spr-5(by101)* mutants declined across generations (Figure 4G), whereas global H3K9me1 and H3K27me2 levels remained unchanged. Although global H3K36me3 was elevated in *spr-5(by101)* mutant worms, it did not change across generations (Figure 4G). Collectively, these findings suggest that the ability of JMJD-2 to regulate H3K9me3 is important and relevant for its effects on the *spr-5* progressive sterility.

A Chromodomain-Containing Gene, *eap-1*, Suppresses Transgenerational *spr-5* Phenotypes

To better understand how H3K9 methylation affects the transgenerational phenotypes of an H3K4me1/me2 demethylase mutant, we carried out an additional targeted fertility RNAi screen in *spr-5(by101)* mutants of 46 genes encoding potential histone methylation recognition modules (Taverna et al., 2007), including PHD, Chromo, MBT repeats, PWWP, or Tudor domains (Figure 5A). Knockdown of the chromodomain-containing gene *cec-3* most potently suppressed the *spr-5* transgenerational fertility defect. We therefore renamed this gene epigenetic memory antagonism protein 1 (*eap-1*). The *eap-1*-null mutant strain (*ok3432*) (confirmed by western blot; Figure S5A), *spr-5;eap-1* double mutants, and wild-type worms laid the same numbers of eggs (Figure 5B). Knockdown or deletion of *eap-1* in *spr-5(by101)* mutant worms also reduced the generational accumulation of H3K4me2 (Figure 5C; data not shown). However, deferred knockdown of *eap-1* beginning at generation 20 failed to revert the transgenerational phenotypes (Figure S4B).

Whole-mount worm immunofluorescence revealed that EAP-1 was expressed in every cell in the embryo (Figure S5B). EAP-1 is predominantly expressed in the head region and the nuclei of the germline (Figures S5C and S5D) where H3K4me2 accumulates in *spr-5* mutants (Nottke et al., 2011). A more detailed examination of EAP-1 expression in dissected gonads revealed that EAP-1 was expressed at all stages throughout the germline (Figures 5D and S5E–S5H).

EAP-1 Binds to Methylated H3K9

The closest mammalian EAP-1 homolog is MPP8 (full length protein: 27.33% identity; chromodomain: 50% identity), which binds methylated H3K9 (Chang et al., 2011; Kokura et al., 2010). In vitro binding assays, using purified chromodomain (EAP-1_{chromo}) or full-length EAP-1 fused to GST, showed that EAP-1 selectively binds to H3K9-methylated peptides (Figures 6A and S6A). Using MPP8 as a guide, we identified F24, W45, and Y48 in EAP-1 as the predicted aromatic cage-forming residues (Chang et al., 2011) (Figure 6A). Mutation of each of these sites to alanine eliminated binding of EAP-1 to H3K9-methylated peptides (Figures 6A and S6B; data not shown). Binding assays using a histone peptide array harboring defined single and combinatorial modifications (Rothbart et al., 2012b) (Table S1) confirmed these findings (Figures S6C and S6D). In the same assay, we found that EAP-1 binding, like the chromodomain of

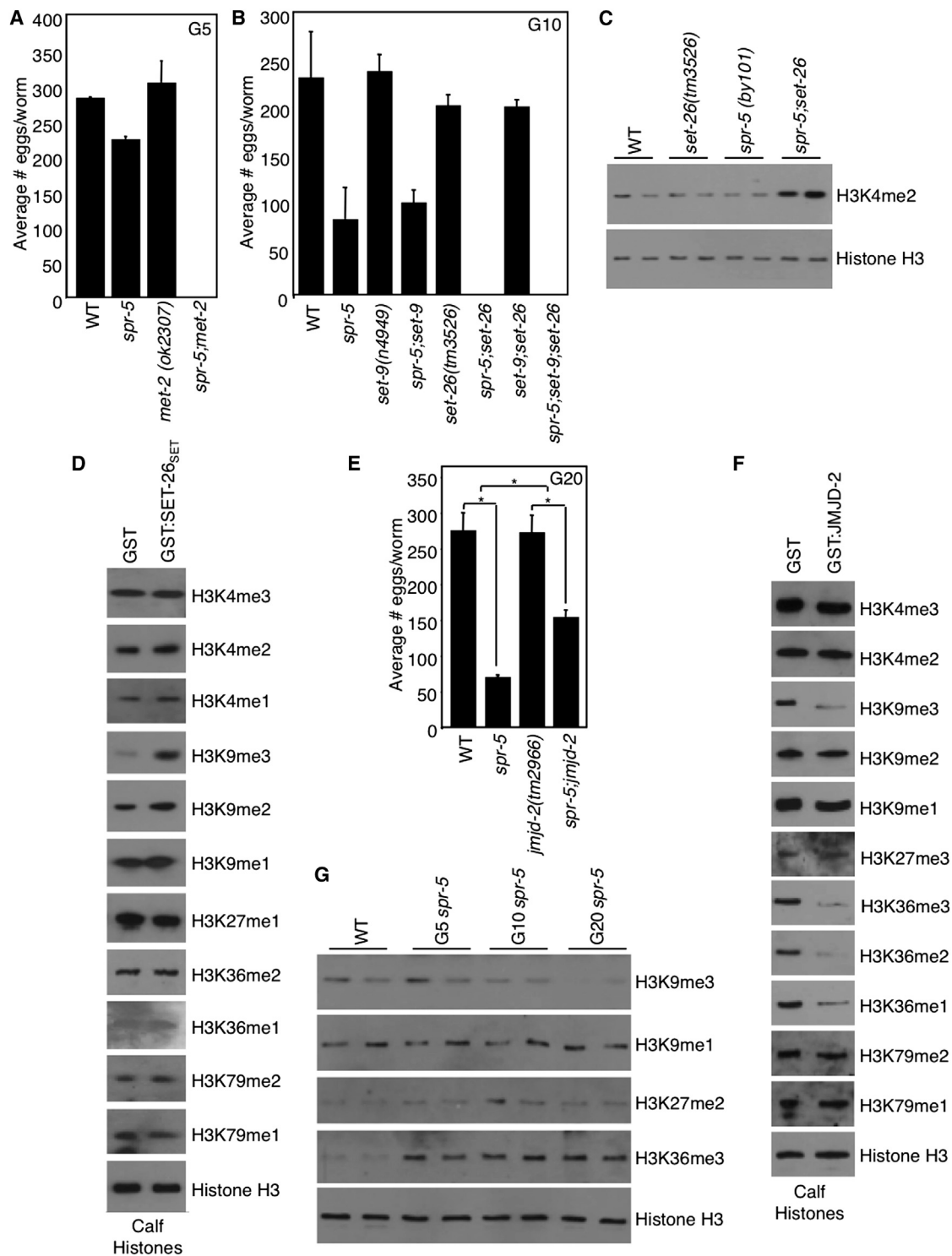


Figure 4. H3K9me Regulation Controls the *spr-5*(by101) Progressive Sterility

(A) *spr-5;met-2* double mutants accelerate the progressive sterility of *spr-5*(by101) mutant worms after five generations. This graph represents the mean \pm SEM of two independent experiments: each experiment consists of average eggs laid for ten worms of each genotype performed in triplicate.

(B) *spr-5;set-26* double mutants accelerate the progressive sterility of *spr-5*(by101) mutant worms after ten generations. Graph is a representative experiment where each bar represents the mean \pm SEM for three replicates of ten worms each. *set-9*(n4949) deletions' effect on fertility has been tested one additional time. *set-26*(tm3526) deletions' effect on fertility has been tested five additional times.

(legend continued on next page)

MPP8 (Rothbart et al., 2012a), was inhibited by phosphorylation of threonine 6 and serine 10 (Figures S6C and S6D).

To assess the affinity of EAP-1 for differentially methylated H3K9, we performed microscale thermophoresis (Jerabek-Willemsen et al., 2011; Wienken et al., 2010) with methyl lysine analog (MLA) histones. EAP-1 bound most tightly to H3K9me3 ($K_d = 157$ nM), followed by H3K9me2 ($K_d = 2.05$ μ M) and H3K9me1 ($K_d = 6.14$ μ M; Figures 6B and S6E). In the same analysis, EAP-1 had no detectable affinity for unmodified histone H3 or H3K4me2 (Figures 6B and S6E). Consistently, we found that, in dissected gonads of wild-type worms, EAP-1 protein signal overlaps with those of H3K9me2/H3K9me3, but not H3K4me1/me2 (Figure 6C). Additionally, deletion of *met-2*, which reduces H3K9me1/H3K9me2 in adults (Bessler et al., 2010), reduced overall EAP-1 chromatin association (Figure 6D). However, deletion of *set-26* had no overt impact on EAP-1 chromatin association globally, suggesting that SET-26 may play a locus-specific methylation role. Collectively, these results identify EAP-1 as an H3K9me reader.

To further examine the mechanistic interaction between EAP-1 and SET-26, we crossed *eap-1(ok3432)* mutants with *set-26(tm3526)* and *spr-5(by101)*. We found that *spr-5; eap-1;set-26* triple mutants laid a similar number of eggs as *spr-5;set-26* double mutants (Figure 7A), suggesting that SET-26 is epistatic to EAP-1.

spr-5 Mutant Worms Lose EAP-1 Binding Across Generations

We next investigated the genomic locations of EAP-1 binding by chromatin immunoprecipitation sequencing (ChIP-seq) experiments on whole worms in wild-type and *spr-5* mutant backgrounds at generations 10 and 20 (Figure 7B). As a control for EAP-1 antibodies, we found no EAP-1 binding in *eap-1(ok3432)*-null mutant worms (data not shown). EAP-1 binding was highest in genomic regions, which had previously been reported to have high H3K9me3 (Gu and Fire, 2010; Liu et al., 2011), consistent with EAP-1 being an H3K9me3 reader. In these regions, EAP-1 binding decreased across the generations (Figure 7B: G0–G10, G10–G20 for regions bound by EAP-1 in wild-type [WT]; $p < 2.2 \times 10^{-16}$), similar to the decline of H3K9me3 seen in western blots of whole worms (Figure 4G). In late-generation *spr-5* mutants, EAP-1 protein level was similar to wild-type worms (Figure S5A) and EAP-1 was still present on chromatin based on immunostaining (data not shown), but EAP-1's binding near the chromosome ends showed a clear decrease (Figure 7B). Together, these results suggest that the decline in EAP-1 enrichment near the chromosome ends over generations may be the consequence of the global decline in H3K9me3 in *spr-5* mutants.

Interestingly, the genes bound by EAP-1 in wild-type worms and in *spr-5* mutants at generation 10 (Table S2) displayed a gene ontology enrichment for regulation of growth ($p = 0.00865346$) and gamete generation ($p = 0.03873372$). An examination of some of the genes in regions of high-EAP-1 binding revealed that their expression increased as EAP-1 binding declined (Figure 7C), consistent with these regions becoming more euchromatic and accessible for transcription. The transgenerationally elevated expression of several of these genes was dependent on *eap-1*, as generation 20 *spr-5;eap-1* double mutant worms had wild-type levels (Figure 7D).

DISCUSSION

In this study, we identified H3K4me1/2 (SET-17 and SET-30) and H3K9me3 methylases (SET-26), as well as an H3K9me3 reader (EAP-1), that regulate transgenerational progressive decline of fertility associated with the persistent loss of the H3K4me1/me2 demethylase *spr-5* in *C. elegans*. Whereas H3K4me2 accumulates, H3K9me3 decreases across the generations of *spr-5* mutants. Our ChIP-seq analysis of the genomic locations of EAP-1 in the *spr-5* mutants suggests a model whereby progressive loss of EAP-1 chromatin association may be important for the transgenerational fertility phenotype associated with SPR-5 loss. Our findings lay the framework for a molecular model where the interplay between H3K4 versus H3K9 methylation impacts transgenerational epigenetic inheritance in *C. elegans*.

spr-5 Mutant Worms Have Reduced Transgenerational Fertility

A recent report (Alvares et al., 2014) suggested that *spr-5(by134)* mutant worms only displayed a transgenerational fertility defect at the elevated temperature of 25°C, but not at 20°C. This result was contrary to the initial results reported by Katz et al. (2009) as well as to our observations. The authors proposed that the transgenerational defect seen by Katz et al. (2009) at 20°C was due to maintaining the *spr-5(by101)* strain as a heterozygous balanced strain or because of potential instability of the *by101 Tc3* transposon insertion. We maintained our strains by crossing repeatedly with a wild-type strain, not as a heterozygous balanced strain, but still observed progressive fertility defects at 20°C (Figure 1A). We also observed a progressive fertility decline in the *spr-5(by134)* strain used by Alvares et al. (2014) at 20°C (Figure S1A). The reduced fecundity of *spr-5* mutant worms was also observed by a third independent group (Kim et al., 2012). Therefore, the discrepancy between the results of Alvares et al. (2014) and those of us and other labs remains unexplained.

(C) *spr-5;set-26* double mutants have significantly higher H3K4me2 at generation 4 as assessed by whole-worm western blots of L3 worms. Representative blot of four independent experiments.

(D) GST:SET-26_{SET} causes an increase in H3K9me2/me3 as assessed by western blots of in vitro methyltransferase assays of histones.

(E) *spr-5;jmjd-2* double-mutant worms have a suppression of the fertility defect of *spr-5(by101)* mutant worms at generation 20 (graph is the mean \pm SEM of three independent experiments: each experiment consists of average eggs laid for ten worms of each genotype performed in triplicate). * $p < 0.05$.

(F) GST:JMJD-2 causes a decrease in H3K9me3 and H3K36me as assessed by western blots of in vitro demethylase assays of histones.

(G) H3K9me3 decreases across generations of *spr-5(by101)* mutant worms as assessed by whole-worm western blots of L4-stage worms. These blots are representative of three independent experiments performed in duplicate.

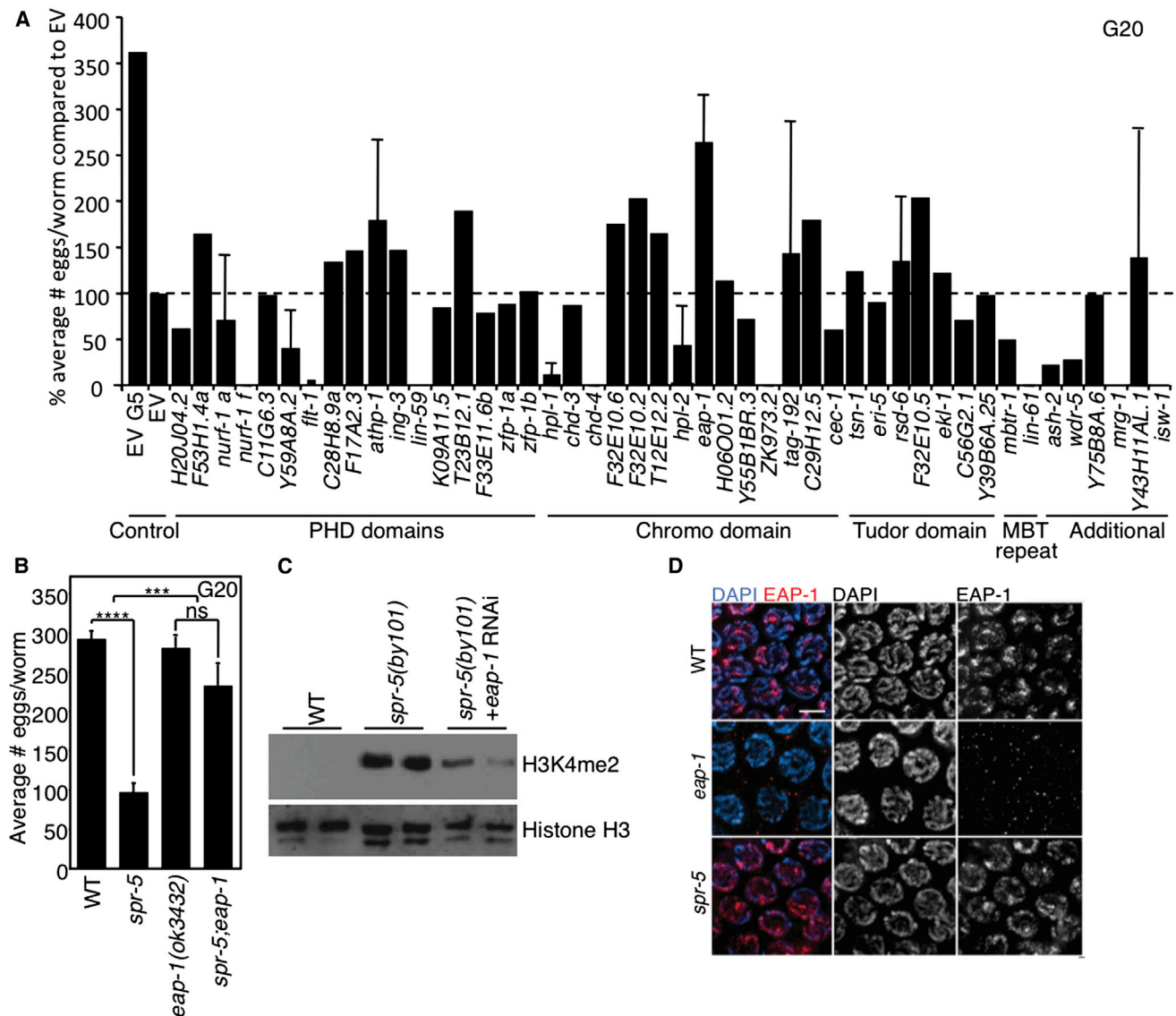


Figure 5. *eap-1* Deletion Suppresses the Progressive Phenotypes of *spr-5* Mutant Worms

(A) *spr-5(by101)* mutant worms fed dsRNA of *C. elegans* potential methyl-binding genes for 20 generations' effect on fertility as compared to EV-treated *spr-5(by101)* mutant worms.

(B) *spr-5;eap-1* double-mutant worms have an almost complete suppression of the fertility defect of *spr-5(by101)* mutant worms at generation 20 (graph is the mean \pm SEM of seven independent experiments: each experiment consists of average eggs laid for ten worms of each genotype performed in triplicate). *** $p < 0.001$, **** $p < 0.0001$.

(C) *spr-5(by101)* mutant worms display increased H3K4me2 at generation 20, which is suppressed by knockdown of *eap-1* for 20 generations as assessed by western blots of whole-worm lysates at the L3 stage.

(D) EAP-1 is expressed in every nucleus throughout the germline and localizes to chromatin as seen in immunofluorescence of midpachytene nuclei of dissected gonads from wild-type, *eap-1(ok3432)*, and *spr-5(by101)* mutants at generation 5.

Suppression versus Reversion of the Transgenerational Phenotypes

Whereas knockdown of *set-17*, *set-30*, or *eap-1* led to suppression of the progressive defects of *spr-5* mutants, only deferred knockdown of *set-30* reverted the phenotypes (Figures 3 and S4). These results suggest that the two H3K4 methyltransferases have both similar and distinct roles in regulating epigenetic inheritance. This difference could be due to differential expression

across cell types, although in situ results suggest both genes are expressed in the germ cells (NEXTDB; <http://nematode.lab.nig.ac.jp>). Alternatively, their functions may be differentially regulated by existing modifications on the histone tails or they may target different genomic loci. Furthermore, their ability to regulate methylation states at H3K4 could be dictated by distinct protein partners. In mammalian cells, DNA methylation is regulated by the de novo methyltransferases DNMT3a/DNMT3b

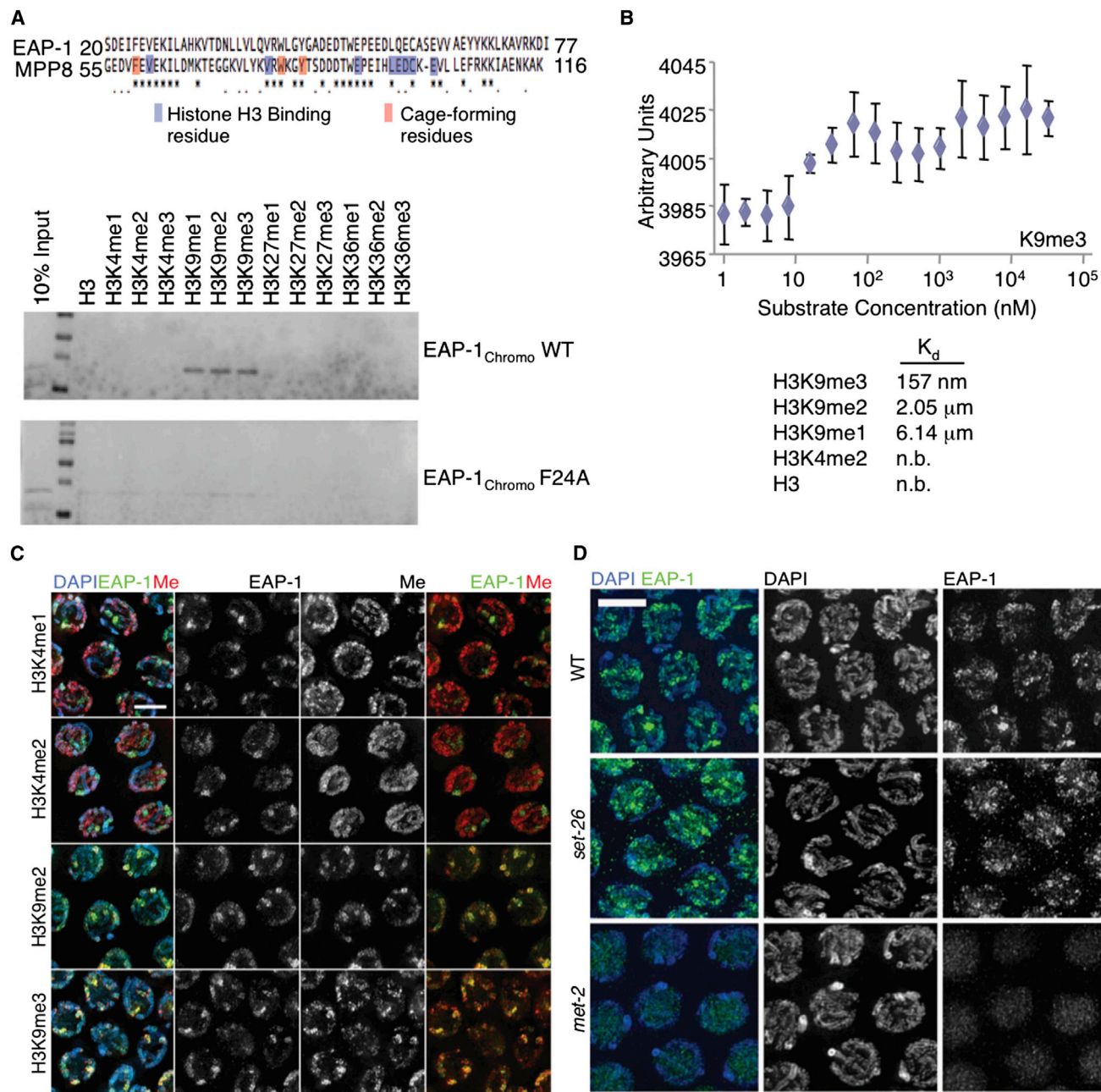


Figure 6. EAP-1 Binds Methylated H3K9

(A) EAP-1_{chromo} binds to H3K9-methylated peptides in *in vitro* binding assays. Shown above is EAP-1 homology to MPP8 with conserved residues marked *. Mutation of any of the three cage-forming amino acids to alanine eliminate EAP-1_{chromo}'s ability to bind to H3K9-methylated peptides (F24A is displayed).

(B) Microscale thermophoresis of EAP-1_{chromo} and MLA histones shows that EAP-1 has highest binding affinity for H3K9me3 than H3K9me2 than H3K9me1 and no binding affinity for H3K4me2 or unmodified histone H3. Binding affinity for H3K9me3 is displayed in the figure, whereas other histone H3 affinities are displayed in Figure S6E.

(C) EAP-1 colocalizes with H3K9me2/H3K9me3, but not with H3K4me1/me2, as assessed by immunofluorescence of dissected gonads from wild-type adult hermaphrodites. Pachytene nuclei are shown. The scale bar represents 4 μ m.

(D) EAP-1 no longer localizes to the chromatin when H3K9 methylation is reduced by mutation of the H3K9me1/me2 methyltransferase *met-2*. Pachytene nuclei are shown. The scale bar represents 4 μ m.

and the maintenance methyltransferase DNMT1 (Bestor, 2000; Okano et al., 1999). Our findings suggest the possibility that, analogous to the mammalian DNA methyltransferases, SET-17

may be required only for maintaining H3K4me1/H3K4me2 levels, whereas SET-30 may be important for both maintaining and resetting the H3K4me2 levels to that of the wild-type worms.

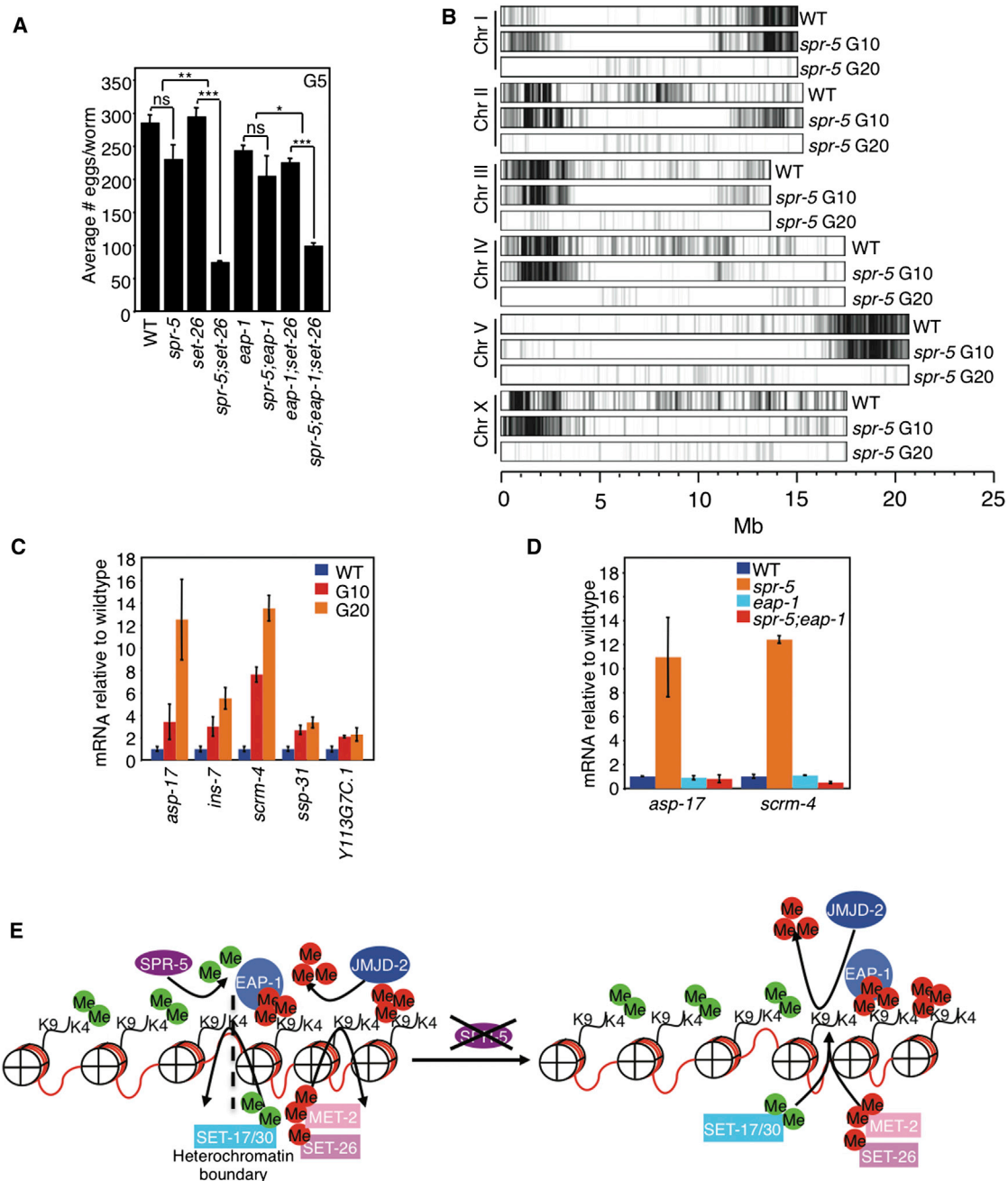


Figure 7. EAP-1 Regulates Transgenerational Gene Expression of *spr-5* Mutant Worms

(A) *spr-5; eap-1; set-26* triple-mutant worms lay as many eggs as *spr-5; set-26* double mutants at generation 5, suggesting that *set-26* is epistatic to *eap-1* (graph is the mean \pm SEM of two independent experiments: each experiment consists of average eggs laid for ten worms of each genotype performed in triplicate). * $p < 0.05$, ** $p < 0.01$, *** $p < 0.001$.

(B) EAP-1 binds to regions that are marked with H3K9me3 and decline across generations of *spr-5*(*by101*) mutant worms. Band intensity reflects EAP-1 binding. Darker regions reflect stronger binding affinity, whereas whiter regions reflect weaker ones. Note that EAP-1 binding does occur in G20 worms but is weaker than in WT and *spr-5* G10 mutant worms.

(C) EAP-1-bound target genes display increases in gene expression across *spr-5*(*by101*) generations. The results represent the mean \pm SD of four biological replicates of \sim 1,000 young adult worms as compared to panactin expression.

(D) EAP-1-bound target genes do not increase in gene expression in generation 20 *spr-5; eap-1* double-mutant worms. The results presented correspond to the mean \pm SEM of two (*scrm-4*) or four (*asp-17*) independent biological experiments of replicates of \sim 1,000 young adult worms as compared to panactin expression.

(E) Model for epigenetic inheritance of elevated H3K4me2.

Potential Molecular Mechanisms

spr-5 mutants display increased global H3K4me2 over generations. Is the altered H3K4me2 itself passed from generation to generation or is the machinery that regulates H3K4 methylation inherited to allow the reacquisition and accumulation of H3K4me2? Recent mammalian cell studies argue for the latter. Specifically, the H3K4 methyltransferase MLL and the polycomb group complexes, PRC1 and PRC2, are either maintained or re-established on chromatin through cell divisions (Blobel et al., 2009; Francis et al., 2009). According to this model, the enzymatic machinery responsible for establishing H3K4me2 states (such as SET-30) could be inherited at specific loci to reapply methyl marks upon DNA duplication.

What might be the molecular mechanisms that underlie the involvement of regulators of both H3K4 and H3K9 methylation in controlling the transgenerational phenotypes associated with the loss of the H3K4me2-specific demethylase SPR-5? We envision three different possibilities that are not mutually exclusive. First, upon loss of SPR-5, H3K4me2 may accumulate randomly, imparting a more open chromatin that is increasingly susceptible to chromatin damage. Indeed, SPR-5 deletion causes perturbation of meiotic DNA double-strand break repair and progressively increased germ cell apoptosis (Nottke et al., 2011). Additionally, PRDM9, the potential homolog of SET-17, has been implicated in mammals as a determinant of appropriate sites of meiotic recombination (Baudat et al., 2013). However, the *spr-5* phenotypes are completely suppressed by adding back a single copy of *spr-5*, suggesting that the transgenerational phenotypes are not due to inherited accumulation of DNA damage. This is consistent with the previous finding that increased H3K9 methylation, rather than H3K4 methylation, correlates with increased mutation rates in human cancer cells (Schuster-Böckler and Lehner, 2012).

Second, H3K4me2 may accumulate by spreading into nearby heterochromatic regions in the absence of SPR-5, thus changing heterochromatin-euchromatin boundaries, which can impact chromatin structure and gene expression. Consistent with this model, in *Drosophila* and *S. pombe*, the homologs of SPR-5 have been shown to play roles in euchromatin-heterochromatin boundary formation (Lan et al., 2007; Rudolph et al., 2007). This is also supported by the global narrowing of EAP-1-binding regions across generations in *spr-5(by101)* mutant worms (Figure 7B). This model, which we favor, predicts that the proteins identified in our screens would function in the same cells to regulate transgenerational inheritance. We therefore propose that, in *C. elegans*, heterochromatic/euchromatin boundaries are maintained by coordinated actions of both the H3K4me1/me2 demethylase SPR-5 and H3K4me1/me2 methyltransferases SET-17 and SET-30 on one side of the equation and the actions of the H3K9me-binding protein EAP-1, the H3K9me3 demethylase JMJD-2, the H3K9me1/me2 methyltransferase MET-2, and the H3K9me3 methyltransferase SET-26 on the other. Thus, loss of SPR-5 may enable the H3K4me2 mark to gradually encroach into the otherwise heterochromatic region (Figure 7E). Supporting this theory, a previous study reported that deletion of the predicted H3K9me1/me2 methyltransferase *met-2* leads to a progressive fertility defect (Andersen and Horvitz, 2007).

This suggests that altering either side of this balanced equation, the H3K4me1/me2 demethylase SPR-5 or the H3K9me1/me2 methyltransferase MET-2 will facilitate euchromatin spreading into heterochromatic regions. Although this second model favors the hypothesis that these proteins function in the same cells, our current data do not preclude the possibility that some of the proteins function in the soma as opposed to the germline to regulate the transgenerational phenotypes after the memory has been transmitted. This alternative scenario could help explain why SET-30, but not SET-17, deletion reverts the progressive fertility defects of *spr-5(by101)* mutant worms.

The third model, which could also explain the misregulation of specific genes involved in fertility regulation, involves SPR-5 impacting local gene expression independently of localized euchromatin expansion. In this scenario, SPR-5 would affect gene expression at specific loci where it is recruited. A previous study reported a misregulation of spermatogenesis genes in *spr-5* mutants (Katz et al., 2009). Similarly, EAP-1-bound genes had a significant enrichment of genes involved in reproduction. Whether these reproduction genes become misregulated through euchromatin expansion or are subject to localized SPR-5 recruitment remains to be determined.

In summary, our findings have revealed a molecular network that controls transgenerational inheritance in *C. elegans* and raise the possibility that perturbation of the balance between histone H3K4 and H3K9 methylation regulation may impact epigenetic inheritance.

EXPERIMENTAL PROCEDURES

All research was performed in accordance with Boston Children's Hospital Institutional Biosafety Committee regulations.

Fertility Assays

From day 3 to day 8 posthatching, ten worms were placed on nematode growth medium plates with OP50-1 in triplicate (30 worms total per condition). Worms were grown at 20°C. However, for initial RNAi screening, only a single plate was used but hits were repeated in triplicate. After 24 hr, the adult worms were removed from each plate and placed on a new plate. The numbers of eggs and hatched worms on the plate were counted. Statistical analyses of fertility were performed using two-way ANOVA tests with Bonferroni posttests or t tests using mean and SE values.

Methyltransferase Assays

Ten micrograms of GST-purified SET-26_{SET}, SET-30, or SET-17 were incubated with histone peptides (amino acids 1–21 of histone H3), recombinant histone H3 (New England Biolabs), histone octamers (Sigma), or nucleosomes purified from 293T cells in the presence of either 0.1 mM S-adenosyl-methionine (SAM) or 2 μCi [³H]SAM at 37°C for 2 hr in a methyltransferase reaction buffer (50 mM Tris-HCl [pH 8.5], 20 mM KCl, 10 mM MgCl₂, 10 mM β-mercaptoethanol, and 250 mM sucrose) as described (Rea et al., 2000). Reactions were subjected to SDS-PAGE and either autoradiography or western blot as described below.

Demethylase Assays

Two micrograms of GST-purified JMJD-2 were incubated with histone octamers (Sigma) at 37°C for 4 hr in a demethylase reaction buffer (20 mM Tris-HCl [pH 7.5], 150 mM NaCl, 50 μM (NH₄)₂Fe(SO₄)₂, 1 mM β-mercaptoethanol, and 2 mM ascorbic acid) as described (Whetstone et al., 2006). Reactions were subjected to SDS-PAGE and western blot as described below.

Microscale Thermophoresis

Fluorescence distribution measurements were taken of fluorescently labeled molecules inside a capillary upon laser irradiation. Temperature gradients were generated by an infrared laser focused on the capillary. Binding affinities are calculated by measuring a temperature jump in the initial stage of irradiation, thermophoretic movement of the molecules within the gradient at later stages, or both (Jerabek-Willemsen et al., 2011; Wienken et al., 2010). At least three independent experiments were performed for each histone modification.

Gonad Dissection, Immunohistochemistry, and Analysis

Gonads from young adult hermaphrodites (24 hr post-L4) were dissected in M9 buffer (22 mM KH₂PO₄, 34 mM K₂HPO₄, 86 mM NaCl, and 1 mM MgSO₄) and fixed on slides with -20°C methanol for 1 min. The remaining steps were carried out at room temperature. Slides were then fixed with 4% formaldehyde (4% formaldehyde in PBS with 80 mM HEPES [pH 7.4], 0.8 mM EDTA, and 1.6 mM MgSO₄) for 30 min. After a 5 min wash in PBS with 0.1% Tween-20, the slides were blocked in 0.5% BSA for 1 hr. Slides were incubated overnight with primary antibodies (α EAP-1, α H3K4me1 [CMA302], α H3K4me2 [CMA303], α H3K9me2 [CMA317], and α H3K9me3 [CMA318]) at a 1:100 dilution. Slides were then incubated with DAPI (Sigma; 1.7 μ g/ml) and secondary antibodies from Jackson ImmunoResearch Laboratories (fluorescein isothiocyanate α rabbit [111-095-144] and Cy3 α mouse [405309]) at a 1:100 dilution for 2 hr.

Images were taken with a 100 \times objective combined with auxiliary magnification (1.6 \times) in 0.2 μ m z stack intervals with an IX-70 microscope (Olympus) and cooled charge-coupled device camera (CH350; Roper Scientific) using the DeltaVision system (Applied Precision). Partial projections of half nuclei are shown.

Additional information about worm strains, constructs, RNA interference, whole-mount immunocytochemistry, genotyping, antibodies, western blotting, peptide-binding assays, ChIP-seq, and real-time analysis can be found in the Supplemental Information section.

ACCESSION NUMBERS

The Gene Expression Omnibus accession number for the ChIP-seq data sets reported in this paper is GSE52102.

SUPPLEMENTAL INFORMATION

Supplemental Information includes Supplemental Discussion, Supplemental Experimental Procedures, six figures, and two tables and can be found with this article online at <http://dx.doi.org/10.1016/j.celrep.2014.02.044>.

AUTHOR CONTRIBUTIONS

E.L.G. and Y.S. conceived and planned the study and wrote the paper. S.E.B.-S. produced Figures 5D, 6C, 6D, and S5E–S5H and was advised by M.P.C. E.B. performed ChIP-seq experiments, helped with the analysis, and produced Figure 7C. R.S. helped produce Figures 4D and S3D. Y.Z. performed ChIP-seq analysis and was advised by W.W. S.B.R. produced Figures S6C and S6D and was advised by B.D.S. S.C. produced Figure 2D. D.A.-C., S.C., and Q.J. helped produce and purify recombinant proteins. A.I.B. performed several western blotting experiments and constructed several plasmids. All authors discussed the results and commented on the manuscript.

ACKNOWLEDGMENTS

We thank T.K. Blackwell, J. Lieberman, and members of the Shi lab for discussions and critical reading of the manuscript. We thank A. Fire for discussions. We thank T. Stiernagle and the Caenorhabditis Genetics Center, which is funded by NIH Office of Research Infrastructure Programs (P40 ODD10440); S. Mitani and the National Bioresource Project for the Experimental Animal “Nematode *C. elegans*”; and D. Moerman laboratories for

C. elegans strains. E.L.G. was supported by T32-CAA009361, a Helen Hay Whitney postdoctoral fellowship, and a National Institute on Aging of the National Institute of Health (NIH) grant (K99AG043550). S.E.B.-S. was supported by an individual NRSA postdoctoral fellowship (F32GM100515) from the NIH/NIGMS, E.B. was supported in part by an EMBO Fellowship, and S.B.R. was supported by the UNC Lineberger Comprehensive Cancer Center Basic Sciences Training Program (T32CA09156) and an American Cancer Society postdoctoral fellowship (PF-13-085-01-DMC). Y.Z. and W.W. were supported in part by an NIH grant (GM096194). B.D.S. was supported in part by an NIH grant (GM068088). M.P.C. was supported by an NIH grant (GM072551), a John and Virginia Kaneb Fellowship, and a grant from the Charles E. W. Grinnell Fund. This work was supported by NIH grants to Y.S. (GM058012, CA118487, and MH096066) and an Ellison Foundation Senior Scholar Award to Y.S. Y.S. is an American Cancer Society Research Professor. Y.S. is also a cofounder of Constellation Pharmaceuticals Inc. and a member of its scientific advisory board.

Received: December 16, 2013

Revised: January 30, 2014

Accepted: February 27, 2014

Published: March 27, 2014

REFERENCES

- Alvares, S.M., Mayberry, G.A., Joyner, E.Y., Lakowski, B., and Ahmed, S. (2014). H3K4 demethylase activities repress proliferative and postmitotic aging. *Aging Cell* 13, 245–253.
- Andersen, E.C., and Horvitz, H.R. (2007). Two *C. elegans* histone methyltransferases repress *lin-3* EGF transcription to inhibit vulval development. *Development* 134, 2991–2999.
- Ashe, A., Sapetschnig, A., Weick, E.M., Mitchell, J., Bagijn, M.P., Cording, A.C., Doebley, A.L., Goldstein, L.D., Lehrbach, N.J., Le Pen, J., et al. (2012). piRNAs can trigger a multigenerational epigenetic memory in the germline of *C. elegans*. *Cell* 150, 88–99.
- Avery, O.T., Macleod, C.M., and McCarty, M. (1944). Studies on the chemical nature of the substance inducing transformation of pneumococcal types: induction of transformation by a desoxyribonucleic acid fraction isolated from pneumococcus type III. *J. Exp. Med.* 79, 137–158.
- Bannister, A.J., Zegerman, P., Partridge, J.F., Miska, E.A., Thomas, J.O., Allshire, R.C., and Kouzarides, T. (2001). Selective recognition of methylated lysine 9 on histone H3 by the HP1 chromo domain. *Nature* 410, 120–124.
- Barski, A., Cuddapah, S., Cui, K., Roh, T.Y., Schones, D.E., Wang, Z., Wei, G., Chepelev, I., and Zhao, K. (2007). High-resolution profiling of histone methylations in the human genome. *Cell* 129, 823–837.
- Baudat, F., Imai, Y., and de Massy, B. (2013). Meiotic recombination in mammals: localization and regulation. *Nat. Rev. Genet.* 14, 794–806.
- Bernstein, B.E., Humphrey, E.L., Erlich, R.L., Schneider, R., Bouman, P., Liu, J.S., Kouzarides, T., and Schreiber, S.L. (2002). Methylation of histone H3 Lys 4 in coding regions of active genes. *Proc. Natl. Acad. Sci. USA* 99, 8695–8700.
- Bessler, J.B., Andersen, E.C., and Villeneuve, A.M. (2010). Differential localization and independent acquisition of the H3K9me2 and H3K9me3 chromatin modifications in the *Caenorhabditis elegans* adult germ line. *PLoS Genet.* 6, e1000830.
- Bestor, T.H. (2000). The DNA methyltransferases of mammals. *Hum. Mol. Genet.* 9, 2395–2402.
- Black, J.C., Allen, A., Van Rechem, C., Forbes, E., Longworth, M., Tschöp, K., Rinehart, C., Quito, J., Walsh, R., Smallwood, A., et al. (2010). Conserved antagonism between JMJD2A/KDM4A and HP1 γ during cell cycle progression. *Mol. Cell* 40, 736–748.
- Blobel, G.A., Kadauke, S., Wang, E., Lau, A.W., Zuber, J., Chou, M.M., and Vakoc, C.R. (2009). A reconfigured pattern of MLL occupancy within mitotic chromatin promotes rapid transcriptional reactivation following mitotic exit. *Mol. Cell* 36, 970–983.

- Capowski, E.E., Martin, P., Garvin, C., and Strome, S. (1991). Identification of grandchildless loci whose products are required for normal germ-line development in the nematode *Caenorhabditis elegans*. *Genetics* *129*, 1061–1072.
- Chang, Y., Horton, J.R., Bedford, M.T., Zhang, X., and Cheng, X. (2011). Structural insights for MPP8 chromodomain interaction with histone H3 lysine 9: potential effect of phosphorylation on methyl-lysine binding. *J. Mol. Biol.* *408*, 807–814.
- Conine, C.C., Moresco, J.J., Gu, W., Shirayama, M., Conte, D., Jr., Yates, J.R., 3rd, and Mello, C.C. (2013). Argonautes promote male fertility and provide a paternal memory of germline gene expression in *C. elegans*. *Cell* *155*, 1532–1544.
- Daxinger, L., and Whitelaw, E. (2012). Understanding transgenerational epigenetic inheritance via the gametes in mammals. *Nat. Rev. Genet.* *13*, 153–162.
- Ebert, A., Lein, S., Schotta, G., and Reuter, G. (2006). Histone modification and the control of heterochromatic gene silencing in *Drosophila*. *Chromosome Res.* *14*, 377–392.
- Francis, N.J., Follmer, N.E., Simon, M.D., Aghia, G., and Butler, J.D. (2009). Polycomb proteins remain bound to chromatin and DNA during DNA replication in vitro. *Cell* *137*, 110–122.
- Greer, E.L., and Shi, Y. (2012). Histone methylation: a dynamic mark in health, disease and inheritance. *Nat. Rev. Genet.* *13*, 343–357.
- Grishok, A., Tabara, H., and Mello, C.C. (2000). Genetic requirements for inheritance of RNAi in *C. elegans*. *Science* *287*, 2494–2497.
- Gu, S.G., and Fire, A. (2010). Partitioning the *C. elegans* genome by nucleosome modification, occupancy, and positioning. *Chromosoma* *119*, 73–87.
- Guenther, M.G., Levine, S.S., Boyer, L.A., Jaenisch, R., and Young, R.A. (2007). A chromatin landmark and transcription initiation at most promoters in human cells. *Cell* *130*, 77–88.
- Hayashi, K., Yoshida, K., and Matsui, Y. (2005). A histone H3 methyltransferase controls epigenetic events required for meiotic prophase. *Nature* *438*, 374–378.
- Heintzman, N.D., Stuart, R.K., Hon, G., Fu, Y., Ching, C.W., Hawkins, R.D., Barrera, L.O., Van Calcar, S., Qu, C., Ching, K.A., et al. (2007). Distinct and predictive chromatin signatures of transcriptional promoters and enhancers in the human genome. *Nat. Genet.* *39*, 311–318.
- Herz, H.M., Garruss, A., and Shilatifard, A. (2013). SET for life: biochemical activities and biological functions of SET domain-containing proteins. *Trends Biochem. Sci.* *38*, 621–639.
- Jerabek-Willemsen, M., Wienken, C.J., Braun, D., Baaske, P., and Duhr, S. (2011). Molecular interaction studies using microscale thermophoresis. *Assay Drug Dev. Technol.* *9*, 342–353.
- Katz, D.J., Edwards, T.M., Reinke, V., and Kelly, W.G. (2009). A *C. elegans* LSD1 demethylase contributes to germline immortality by reprogramming epigenetic memory. *Cell* *137*, 308–320.
- Kim, S., Govindan, J.A., Tu, Z.J., and Greenstein, D. (2012). SACY-1 DEAD-Box helicase links the somatic control of oocyte meiotic maturation to the sperm-to-oocyte switch and gamete maintenance in *Caenorhabditis elegans*. *Genetics* *192*, 905–928.
- Klose, R.J., Kallin, E.M., and Zhang, Y. (2006). JmjC-domain-containing proteins and histone demethylation. *Nat. Rev. Genet.* *7*, 715–727.
- Kokura, K., Sun, L., Bedford, M.T., and Fang, J. (2010). Methyl-H3K9-binding protein MPP8 mediates E-cadherin gene silencing and promotes tumour cell motility and invasion. *EMBO J.* *29*, 3673–3687.
- Lan, F., Zaratiegui, M., Villén, J., Vaughn, M.W., Verdel, A., Huarte, M., Shi, Y., Gygi, S.P., Moazed, D., Martienssen, R.A., and Shi, Y. (2007). *S. pombe* LSD1 homologs regulate heterochromatin propagation and euchromatic gene transcription. *Mol. Cell* *26*, 89–101.
- Li, B., Carey, M., and Workman, J.L. (2007). The role of chromatin during transcription. *Cell* *128*, 707–719.
- Liu, T., Rechtsteiner, A., Egelhofer, T.A., Vielle, A., Latorre, I., Cheung, M.S., Ercan, S., Ikegami, K., Jensen, M., Kolasinska-Zwiercz, P., et al. (2011). Broad chromosomal domains of histone modification patterns in *C. elegans*. *Genome Res.* *21*, 227–236.
- Mikkelsen, T.S., Ku, M., Jaffe, D.B., Issac, B., Lieberman, E., Giannoukos, G., Alvarez, P., Brockman, W., Kim, T.K., Koche, R.P., et al. (2007). Genome-wide maps of chromatin state in pluripotent and lineage-committed cells. *Nature* *448*, 553–560.
- Moazed, D. (2011). Mechanisms for the inheritance of chromatin states. *Cell* *146*, 510–518.
- Mosammaparast, N., and Shi, Y. (2010). Reversal of histone methylation: biochemical and molecular mechanisms of histone demethylases. *Annu. Rev. Biochem.* *79*, 155–179.
- Ni, Z., Ebata, A., Alipanahramandi, E., and Lee, S.S. (2012). Two SET domain containing genes link epigenetic changes and aging in *Caenorhabditis elegans*. *Aging Cell* *11*, 315–325.
- Nottke, A.C., Beese-Sims, S.E., Pantalena, L.F., Reinke, V., Shi, Y., and Colaiacovo, M.P. (2011). SPR-5 is a histone H3K4 demethylase with a role in meiotic double-strand break repair. *Proc. Natl. Acad. Sci. USA* *108*, 12805–12810.
- Okano, M., Bell, D.W., Haber, D.A., and Li, E. (1999). DNA methyltransferases Dnmt3a and Dnmt3b are essential for de novo methylation and mammalian development. *Cell* *99*, 247–257.
- Pokholok, D.K., Harbison, C.T., Levine, S., Cole, M., Hannett, N.M., Lee, T.I., Bell, G.W., Walker, K., Rolfe, P.A., Herbolsheimer, E., et al. (2005). Genome-wide map of nucleosome acetylation and methylation in yeast. *Cell* *122*, 517–527.
- Rea, S., Eisenhaber, F., O’Carroll, D., Strahl, B.D., Sun, Z.W., Schmid, M., Opravil, S., Mechtler, K., Ponting, C.P., Allis, C.D., and Jenuwein, T. (2000). Regulation of chromatin structure by site-specific histone H3 methyltransferases. *Nature* *406*, 593–599.
- Rothbart, S.B., Krajewski, K., Nady, N., Tempel, W., Xue, S., Badeaux, A.I., Barsyte-Lovejoy, D., Martinez, J.Y., Bedford, M.T., Fuchs, S.M., et al. (2012a). Association of UHRF1 with methylated H3K9 directs the maintenance of DNA methylation. *Nat. Struct. Mol. Biol.* *19*, 1155–1160.
- Rothbart, S.B., Krajewski, K., Strahl, B.D., and Fuchs, S.M. (2012b). Peptide microarrays to interrogate the “histone code”. *Methods Enzymol.* *512*, 107–135.
- Rudolph, T., Yonezawa, M., Lein, S., Heidrich, K., Kubicek, S., Schäfer, C., Phalke, S., Walther, M., Schmidt, A., Jenuwein, T., and Reuter, G. (2007). Heterochromatin formation in *Drosophila* is initiated through active removal of H3K4 methylation by the LSD1 homolog SU(VAR)3-3. *Mol. Cell* *26*, 103–115.
- Ruthenburg, A.J., Allis, C.D., and Wysocka, J. (2007). Methylation of lysine 4 on histone H3: intricacy of writing and reading a single epigenetic mark. *Mol. Cell* *25*, 15–30.
- Santos-Rosa, H., Schneider, R., Bannister, A.J., Sherriff, J., Bernstein, B.E., Emre, N.C., Schreiber, S.L., Mellor, J., and Kouzarides, T. (2002). Active genes are tri-methylated at K4 of histone H3. *Nature* *419*, 407–411.
- Schuster-Böckler, B., and Lehner, B. (2012). Chromatin organization is a major influence on regional mutation rates in human cancer cells. *Nature* *488*, 504–507.
- Taverna, S.D., Li, H., Ruthenburg, A.J., Allis, C.D., and Patel, D.J. (2007). How chromatin-binding modules interpret histone modifications: lessons from professional pocket pickers. *Nat. Struct. Mol. Biol.* *14*, 1025–1040.
- Towbin, B.D., González-Aguilera, C., Sack, R., Gaidatzis, D., Kalck, V., Meister, P., Askjaer, P., and Gasser, S.M. (2012). Step-wise methylation of histone H3K9 positions heterochromatin at the nuclear periphery. *Cell* *150*, 934–947.
- Wang, Z., Zang, C., Rosenfeld, J.A., Schones, D.E., Barski, A., Cuddapah, S., Cui, K., Roh, T.Y., Peng, W., Zhang, M.Q., and Zhao, K. (2008). Combinatorial patterns of histone acetylations and methylations in the human genome. *Nat. Genet.* *40*, 897–903.
- Whetstone, J.R., Nottke, A., Lan, F., Huarte, M., Smolnikov, S., Chen, Z., Spooner, E., Li, E., Zhang, G., Colaiacovo, M., and Shi, Y. (2006). Reversal of histone

lysine trimethylation by the JMJD2 family of histone demethylases. *Cell* 125, 467–481.

Wienken, C.J., Baaske, P., Rothbauer, U., Braun, D., and Duhr, S. (2010). Protein-binding assays in biological liquids using microscale thermophoresis. *Nat. Commun.* 1, 100.

Yigit, E., Batista, P.J., Bei, Y., Pang, K.M., Chen, C.C., Tolia, N.H., Joshua-Tor, L., Mitani, S., Simard, M.J., and Mello, C.C. (2006). Analysis of the *C. elegans* Argonaute family reveals that distinct Argonautes act sequentially during RNAi. *Cell* 127, 747–757.

Youngson, N.A., and Whitelaw, E. (2008). Transgenerational epigenetic effects. *Annu. Rev. Genomics Hum. Genet.* 9, 233–257.